

# ROLAIDS-CPM: A CODE FOR ACCURATE RESONANCE ABSORPTION CALCULATIONS

W.J.M. DE KRUIJF



The Netherlands Energy Research Foundation ECN is the leading institute in the Netherlands for energy research. ECN carries out basic and applied research in the fields of nuclear energy, fossil fuels, renewable energy sources, policy studies, environmental aspects of energy supply and the development and application of new materials.

ECN employs more than 900 staff. Contracts are obtained from the government and from national and foreign organizations and industries.

ECN's research results are published in a number of report series, each series serving a different public, from contractors to the international scientific world.

The R-series is for research reports that make the results of ECN research available to the international technical and scientific world.

Het Energieonderzoek Centrum Nederland (ECN) is het centrale instituut voor onderzoek op energiegebied in Nederland. ECN verricht fundamenteel en toegepast onderzoek op het gebied van kernenergie, fossiele-energiedragers, duurzame energie, beleidsstudies, milieuaspecten van de energievoorziening en de ontwikkeling en toepassing van nieuwe materialen.

Bij ECN zijn ruim 900 medewerkers werkzaam. De opdrachten worden verkregen van de overheid en van organisaties en industrieën uit binnen- en buitenland.

De resultaten van het ECN-onderzoek worden neergelegd in diverse rapportenseries, bestemd voor verschillende doelgroepen, van opdrachtgevers tot de internationale wetenschappelijke wereld.

De R-serie is de serie research-rapporten die de resultaten van ECN-onderzoek toegankelijk maken voor de internationale technisch-wetenschappelijke wereld.

Netherlands Energy Research Foundation ECN  
P.O. Box 1  
NL-1755 ZG Petten  
the Netherlands  
Telephone : +31 2246 49 49  
Fax : +31 2246 44 80

This report is available on remittance of Dfl. 35 to:  
ECN, General Services,  
Petten, the Netherlands  
Postbank account No. 3977703.  
Please quote the report number.

© Netherlands Energy Research Foundation ECN

Energieonderzoek Centrum Nederland  
Postbus 1  
1755 ZG Petten  
Telefoon : (02246) 49 49  
Fax : (02246) 44 80

Dit rapport is te verkrijgen door het overmaken van f 35,- op girorekening 3977703 ten name van:  
ECN, Algemene Diensten  
te Petten  
onder vermelding van het rapportnummer.

© Energieonderzoek Centrum Nederland

# ROLAIDS-CPM: A CODE FOR ACCURATE RESONANCE ABSORPTION CALCULATIONS

W.J.M. DE KRIJF

## **Abstract**

ROLAIDS is used to calculate group-averaged cross sections for specific zones in a one-dimensional geometry. This report describes ROLAIDS-CPM which is an extended version of ROLAIDS. The main extension in ROLAIDS-CPM is the possibility to use the collision probability method for a slab- or cylinder-geometry instead of the less accurate interface-currents method. In this way accurate resonance absorption calculations can be performed with ROLAIDS-CPM. ROLAIDS-CPM has been developed at ECN.

## **Keywords**

ROLAIDS-CPM

Collision Probability Method

Resonance Absorption

# CONTENTS

SUMMARY	5
1. INTRODUCTION	7
2. THEORY	8
2.1 Introduction	8
2.2 Slowing Down Treatment	8
2.3 Interface-Currents Method	9
2.4 Collision Probability Method	10
2.4.1 Introduction	10
2.4.2 General	11
2.4.3 Slab-Geometry	12
2.4.4 Cylinder-Geometry	13
2.5 Calculation of effective cross sections	17
3. POSITION OF ROLAIDS-CPM IN CODE SYSTEM	18
4. INPUT DESCRIPTION	21
4.1 Introduction	21
4.2 Data Block 1	21
4.2.1 0\$\$Array[10]	21
4.2.2 1\$\$Array[6]	22
4.2.3 2\$\$Array[8]	23
4.2.4 3\$\$Array[2]	23
4.2.5 4\$\$Array[6]	24
4.3 Data Block 2	24
5. CONCLUSION	25
REFERENCES	26

# SUMMARY

ROLAIDS is used to calculate group-averaged cross sections for specific zones in a one-dimensional geometry. This report describes ROLAIDS-CPM which is an extended version of ROLAIDS. The main extension in ROLAIDS-CPM is the possibility to use the collision probability method for a slab- or cylinder-geometry instead of the less accurate interface-currents method. In this way accurate resonance absorption calculations can be performed with ROLAIDS-CPM.

# 1. INTRODUCTION

Resonance absorption is an important phenomenon in nuclear reactors. Much effort is done to calculate resonance absorption accurately. Because of the strong dependence of the resonance cross section on the energy, the calculation of resonance absorption is not straightforward.

We are primarily interested in the calculation of resonance absorption in a simple one-dimensional unit-cell. Resonance absorption effects in such a unit-cell are generally calculated by multigroup transport lattice codes. These codes use cross sections which have been averaged over an energy group. When the cross section hardly varies over an energy group, the calculation of a group-averaged or effective cross section is quite easy. However, one energy group may contain one or more resonances of one or more nuclides. A lot of methods exist to calculate effective cross sections which should be used in the multigroup transport calculation to arrive at correct resonance absorption rates [1-5].

In the framework of a PhD project on detailed calculations of the fuel temperature effect in an LWR fuel pin, the influence of the radial temperature profile in a fuel pin is to be investigated. Not only the total absorption in a fuel pin, but also the distribution of the absorption over the fuel pin has to be calculated correctly. Because of the spatial dependence of the flux group-averaged cross sections at the center of the fuel pin should differ from the group-averaged cross sections at the surface of the fuel-pin. Therefore, codes which calculate group-averaged cross sections for the fuel pin as a whole [1,2] cannot be used for this purpose. Other codes [3-5] cannot treat resonance overlap between resonances of the same nuclide at different temperatures.

These drawbacks are not present in ROLAIDS [6,7]. ROLAIDS is a code of the AMPX code system [8] and stands for Resonance OverLap Analysis In Discretely represented Systems. ROLAIDS uses energy-pointwise cross sections and produces group-averaged cross sections for so-called "superzones".

This report describes ROLAIDS-CPM which is an extended version of ROLAIDS. The extension CPM stands for Collision Probability Method. Whereas ROLAIDS assumes cosine currents at the interfaces of the zones, ROLAIDS-CPM does not need this assumption. In fact, ROLAIDS-CPM calculates resonance absorption directly from the energy-pointwise cross sections; it does not need a subsequent multigroup transport calculation. The theory behind ROLAIDS-CPM is described in chapter 2.

The position of ROLAIDS-CPM in the code package at ECN as well as the program PIR that produces the input-library for ROLAIDS-CPM is described in chapter 3. The input prescription for ROLAIDS-CPM is given in chapter 4.

The names ROLAIDS and ROLAIDS-CPM are both used in this report. ROLAIDS-CPM is just an extension of ROLAIDS. The name ROLAIDS is used when the description is also valid for the original ROLAIDS.

## 2. THEORY

### 2.1 Introduction

ROLAIDS performs an energy-pointwise slowing down integral transport calculation in one-dimensional geometry. Section 2.2 explains the slowing down treatment. Section 2.3 describes the interface-currents method which is used in ROLAIDS to perform the integral transport calculation. Section 2.4 describes the major extension in ROLAIDS-CPM: the collision probability method to perform the integral transport calculation.

### 2.2 Slowing Down Treatment

ROLAIDS uses an energy-pointwise cross section library. It reads the elastic scattering cross section (MT=2), the fission cross section (MT=18), and the radiative capture cross section (MT=102) from this library. Because ROLAIDS assumes elastic scattering (isotropic in the CM system), the highest energy for which ROLAIDS can be used is limited by the onset of inelastic scattering. At low energies ROLAIDS is limited by thermal upscattering.

ROLAIDS defines the total cross section as the sum of MT=2,18, and 102. Because ROLAIDS uses MT=102 and not MT=101, which is the total neutron disappearance cross section, care should be taken that the only significant contribution to the neutron disappearance is radiative capture. When this is not the case one might play a trick upon ROLAIDS by redefining the meaning of the MT numbers. One might for example put a second significant contribution to the neutron disappearance for non-fissionable nuclei on the library with MT=18. Or one might construct the energy-pointwise MT=101 cross section and put it on the library with MT=102. However, one should be careful with the further usage of the effective cross sections calculated by ROLAIDS. They should get the correct MT number again.

ROLAIDS forms a pointwise energy mesh which consists of the group boundaries of the AMPX-M library for which shielded cross sections are calculated, the group boundaries of the GAM-II group structure, and all the mesh points present on the energy-pointwise library. Furthermore, it inserts an energy mesh based on the maximum scattering interval for a scattering collision with the heaviest nuclide. ROLAIDS-CPM has the option to insert an energy mesh based on half of this maximum scattering interval. This is done to have enough energy-points in the energy-range where the cross sections hardly vary.

The energy mesh is cleaned by deleting energy-points which are too close to other points according to the next equation:

$$\frac{|E_i - E_j|}{E_j} < \epsilon, \quad (1)$$

where  $E_i$  is an energy-point,  $E_j$  a possible new energy-point, and  $\epsilon$  the value below which energy-points are deleted. ROLAIDS-CPM has the possibility to vary the value of  $\epsilon$ . The default value is  $1E-5$  (as in ROLAIDS).

ROLAIDS assumes a spatially flat  $\frac{1}{E}$  flux above the highest energy of the problem. In addition, ROLAIDS-CPM has an option to use a spatially flat  $\frac{1}{E}$  source in



specific zones between a specified energy and the highest energy of the problem. The source is normalized to 1. This option has been built in to use ROLAIDS-CPM in a calculational benchmark [9].

Assuming elastic scattering, isotropic in the CM system, the number of neutrons per unit of time and energy slowing down to energy  $E_i$  in zone  $j$  is given by:

$$S_{i,j} = \sum_m \frac{N_{j,m}}{(1 - \alpha_m)} \cdot \int_{V_j} \int_{E_i}^{\frac{E_i}{\alpha_m}} \frac{\phi_j(E') \cdot \sigma_{sm}(E')}{E'} \cdot dE' \cdot dV, \quad (2)$$

where  $N_{j,m}$  is the density of nuclide  $m$  in zone  $j$ ,  $V_j$  the volume of zone  $j$ ,  $\phi_j$  the flux in zone  $j$ ,  $\sigma_{sm}$  the microscopic scattering cross section for nuclide  $m$ , and

$$\alpha_m = \left( \frac{AWR - 1}{AWR + 1} \right)^2, \quad (3)$$

where  $AWR$  is the atomic weight ratio for nuclide  $m$  which about equals the nuclear mass number  $A$ .

The scattering rate is assumed to vary linearly between the energy-points. The slowing down source as given by equation 2 can be evaluated according to:

$$S_{i,j} = \sum_k a_{k,j} \cdot C_{k,j} \quad (4)$$

$$= a_{i,j} \cdot C_{i,j} + \sum_{k < i} a_{k,j} \cdot C_{k,j}, \quad (5)$$

where  $a_{k,j}$  is the coefficient for the contribution of the collision rate  $C_{k,j}$  in zone  $j$  at energy  $k$  to the source  $S_{i,j}$  resulting from the evaluation of equation 2. The first term on the righthandside of equation 5 has been taken apart because the collision rate at energy  $i$  is calculated from the sources at energy  $i$  which are not known yet.

Before actually performing the slowing down calculation, ROLAIDS sets up a data file which contains all the necessary information for the calculation of the slowing down sources in the specific energy-range. This file is independent of the problem geometry.

An important extension of ROLAIDS-CPM for our purpose is the ability to use one nuclide at different temperatures in the same problem. This extension has been based on some book-keeping.

## 2.3 Interface-Currents Method

For convenience, suppose that the coefficient  $a_{i,j}$  in the first term on the righthand-side of equation 5 is zero. This is not essential for the interface-currents method, but facilitates a better understanding of the equations involved. The complete equations are given in [6]. The slowing down source can now directly be calculated from previously calculated collision rates at higher energies. The subscript  $i$  for the energy has been omitted in the rest of this section. We will demonstrate the method for a slab-geometry.

Figure 2.1 defines the in- and out-going currents for a specific zone  $j$ .

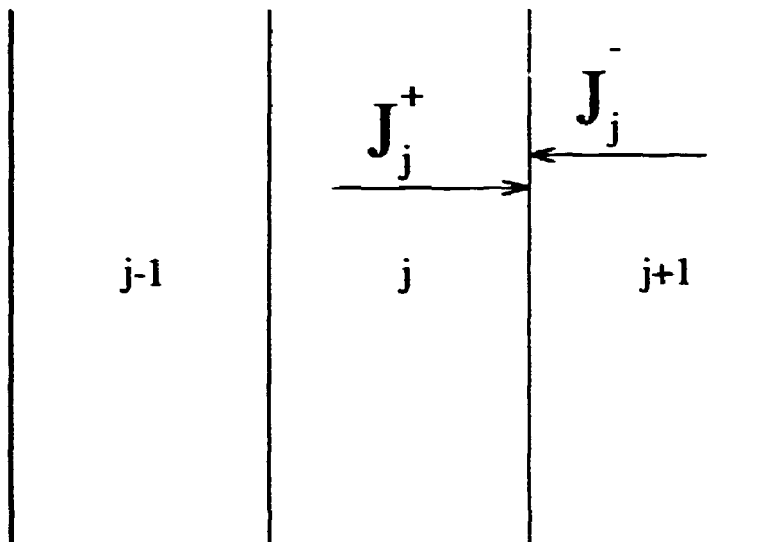


Figure 2.1 Definition of the in- and out-going currents for zone  $j$ .

The currents  $J_j^+$  and  $J_j^-$  are calculated according to:

$$J_j^+ = J_{j-1}^+ \cdot T_j + 0.5 \cdot S_j \cdot P_j, \quad (6)$$

$$J_j^- = J_{j+1}^- \cdot T_j + 0.5 \cdot S_{j+1} \cdot P_{j+1}, \quad (7)$$

where  $T_j$  is the probability for a neutron from a cosine current at the boundary of zone  $j$  to arrive without collision at the other boundary of the zone,  $S_j$  the source in zone  $j$ , and  $P_j$  the escape probability for a spatially flat isotropic source in zone  $j$ . A cosine current means that the flux is half-isotropic so that the current is linear with the cosine of the angle with the normal at the boundary.

The assumption of cosine currents and spatially flat isotropic sources facilitates the analytic evaluation of the transmission and escape probabilities [7].

When the currents have been calculated, the collision rates  $C_j$  follow from:

$$C_j = (1 - T_j) \cdot J_j^- + (1 - T_j) \cdot J_{j-1}^+ + (1 - P_j) \cdot S_j. \quad (8)$$

These collision rates are used to calculate the scattering sources to lower energies according to equation 2.

For the zones at the boundary of the specified problem the equations depend on the boundary conditions.

## 2.4 Collision Probability Method

### 2.4.1 Introduction

The assumption of spatially flat sources in the different zones is not a real physical limitation because the effect of this assumption can be made very small by taking more zones into account.

The assumption of isotropic sources in the LAB-system however is a physical limitation of ROLAIDS but this assumption is not expected to have much effect in the calculation of resonance absorption effects. The scattering in the moderator is mainly isotropic because the flux in the moderator is mainly isotropic and the

scattering in the fuel is mainly isotropic because of the large mass numbers of the nuclides in the fuel. The influence of this assumption can be investigated with multigroup lattice codes which can handle non-isotropic scattering in the LAB-system.

The assumption of cosine currents at the interfaces of the zones is a more serious physical limitation. When the distribution of the absorption over the fuel pin is wanted, the fuel has to be divided in different zones. The currents at the interfaces of the zones in the fuel do not have a cosine profile at the resonance energies. This can be seen best in a slab-geometry where the currents will be strongly forwards peaked. A finer discretization of the spatial mesh only makes things worse because the assumption is made at every interface. To overcome the assumption of cosine currents at the interfaces of the zones the collision probability method has been implemented in ROLAIDS-CPM.

## 2.4.2 General

The collision rate in zone  $j$  at energy  $i$  is given by:

$$C_{i,j} = \sum_{l=1}^N P_{i,j,l} \cdot S_{i,l}, \quad (9)$$

where  $P_{i,j,l}$  is the probability for a neutron with energy  $E_i$  from a spatially flat isotropic source in zone  $l$  to have its first collision in zone  $j$ . When equation 5 is substituted in equation 9 we get:

$$C_{i,j} = \sum_{l=1}^N P_{i,j,l} \cdot a_{i,l} \cdot C_{i,l} + \sum_{l=1}^N P_{i,j,l} \cdot \sum_{k < i} a_{k,l} \cdot C_{k,l}. \quad (10)$$

The second term of this equation can easily be evaluated, but the first term is more difficult. The collision rate in zone  $j$  at energy  $i$  depends directly on the collision rates at energy  $i$  in all other zones. This term is called the self-scatter term because it involves neutrons which hardly lose energy in a scattering collision. Because of the fine energy mesh that is used this term will be very small and solving equation 10 exactly would mean overdoing it a bit. Instead we use a simple iteration scheme which is stopped after the first iteration because of the expected very good convergence. First, we obtain a good initial guess by making the following assumption for the collision probabilities of the self-scatter term:

$$P_{i,j,l} = 1 \quad j = l, \quad (11)$$

$$P_{i,j,l} = 0 \quad j \neq l. \quad (12)$$

This simplifies equation 10 to:

$$C'_{i,j} = a_{i,j} \cdot C'_{i,j} + \sum_{l=1}^N P_{i,j,l} \cdot \sum_{k < i} a_{k,l} \cdot C_{k,l}, \quad (13)$$

where  $C'_{i,j}$  is the collision rate which follows from this simplified equation.

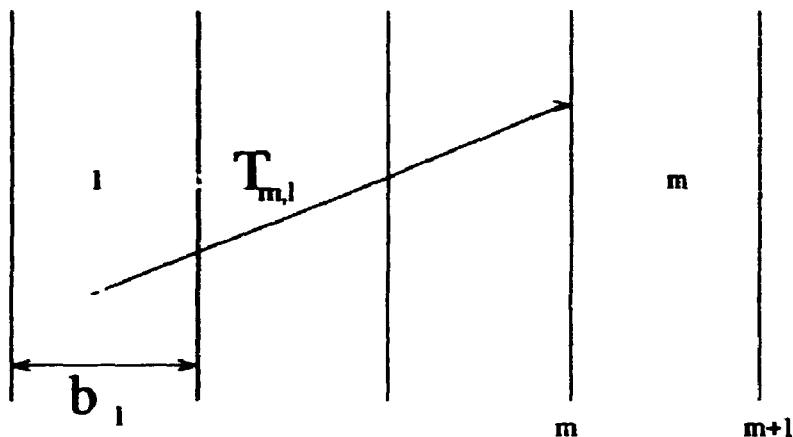


Figure 2.2 Transmission probability in slab-geometry.

This assumption physically means that neutrons which hardly lose energy in a scattering collision have their next collision in the same zone. Then, after the first and only iteration step, the self-scatter terms are given by:

$$C_{ij}^{self} = \sum_{l=1}^N P_{i,j,l} \cdot a_{i,l} \cdot C_{i,l}, \quad (14)$$

and the collision rates are given by:

$$C_{ij} = C_{ij}' \cdot (1 - a_{ij}) + C_{ij}^{self}. \quad (15)$$

We turn our attention to the calculation of the collision probabilities. The collision probability method has been built in for the slab- and cylinder-geometries. In the next subsections the subscript for the energy has been omitted.

### 2.4.3 Slab-Geometry

The probability for a neutron from a spatially flat isotropic source in zone  $l$  to escape to the boundary  $m$ ,  $T_{m,l}$ , is given by:

$$T_{m,l} = \frac{1}{2 \cdot \Sigma_{t,l} \cdot b_l} \cdot \left( E_3 \left( \sum_{j>l}^{j<m} \Sigma_{t,j} \cdot b_j \right) - E_3 \left( \sum_{j>l} \Sigma_{t,j} \cdot b_j + b_l \cdot \Sigma_{t,l} \right) \right), \quad (16)$$

where  $\Sigma_{t,j}$  is the total macroscopic cross section in zone  $j$ ,  $b_j$  the width of zone  $j$  and  $E_3(x)$  the exponential integral function of order 3. Figure 2.2 shows the geometry.

The collision probability  $P_{m,l}$  with  $m > l$  is given by:

$$P_{m,l} = T_{m,l} - T_{m+1,l}. \quad (17)$$

The collision probability method for the slab-geometry has been built in with a reflective or a periodic boundary condition.

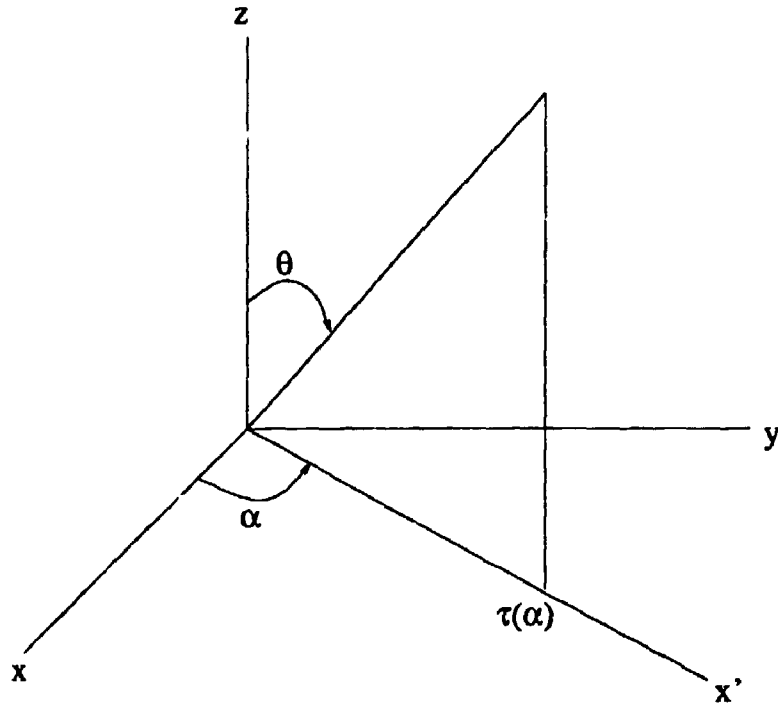


Figure 2.3 Probability for neutron to travel "horizontal" distance  $\tau$ .

#### 2.4.4 Cylinder-Geometry

The method of calculating the collision probabilities in cylinder-geometry will be described in more detail. The calculation is completely based on Carlvik's method [10].

First, consider neutrons from a line source along the  $z$ -axis which are isotropically emitted in a small azimuthal angle  $d\alpha$  between  $\theta = 0$  and  $\theta = \pi$ , where  $\theta$  is defined as the angle with the  $z$ -axis. The space angle is given by:  $\int_0^\pi \sin\theta d\theta d\alpha = 2 \cdot d\alpha$ . Figure 2.3 illustrates the problem which is invariant in the  $z$ -direction. The probability  $P(\tau)$  that a source neutron will travel so far without colliding that the projection of the path on the plane perpendicular to the line source is at least  $\tau$ , where  $\tau$  is measured in optical units, is given by:

$$P(\tau) = \frac{1}{2 \cdot d\alpha} \int_0^\pi \exp\left(-\frac{\tau}{\sin\theta}\right) \sin\theta d\theta d\alpha = Ki_2(\tau), \quad (18)$$

where  $Ki_n(x)$  is the Bickley function of order  $n$  [11].

Next, we turn to a general two-dimensional problem which is illustrated by figure 2.4. Again, those neutrons are considered which are emitted in a small azimuthal angle  $d\alpha$  between  $\theta = 0$  and  $\theta = \pi$ , where  $\theta$  is the angle with the  $z$ -axis. The probability for neutrons which start homogeneously along a line  $x'$  in space angle  $2 \cdot d\alpha$  in zone  $l$  to collide in zone  $j$  is given by:

$$P_{j,l}(y') = \frac{1}{a(y')} \int_0^{a(y')} [Ki_2(\Sigma_{t_l}(a - x') + \tau_{j,l}) - Ki_2(\Sigma_{t_l}(a - x') + \tau_{j,l} + \tau_j)] dx' = \frac{1}{\Sigma_{t_l} \cdot a(y')} [Ki_3(\tau_{j,l}) - Ki_3(\tau_{j,l} + \tau_l) - Ki_3(\tau_{j,l} + \tau_j) + Ki_3(\tau_{j,l} + \tau_l + \tau_j)]. \quad (19)$$

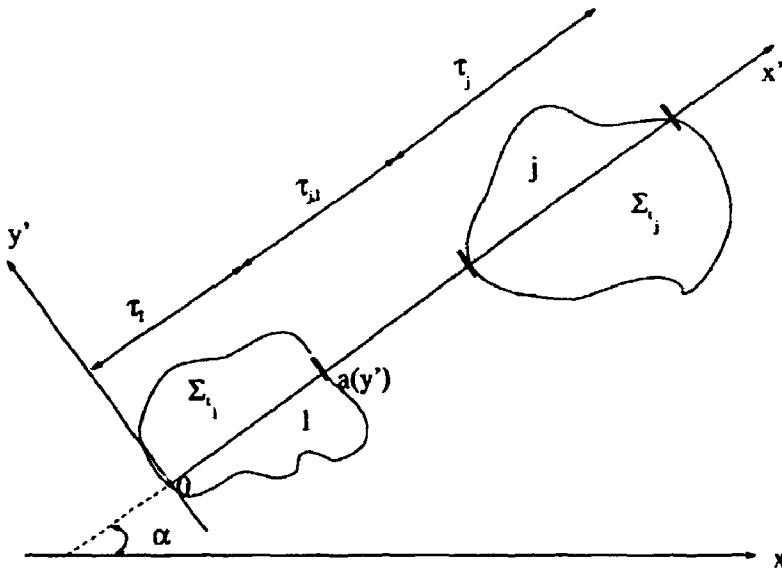


Figure 2.4 Calculation of collision probabilities in general two-dimensional geometry.

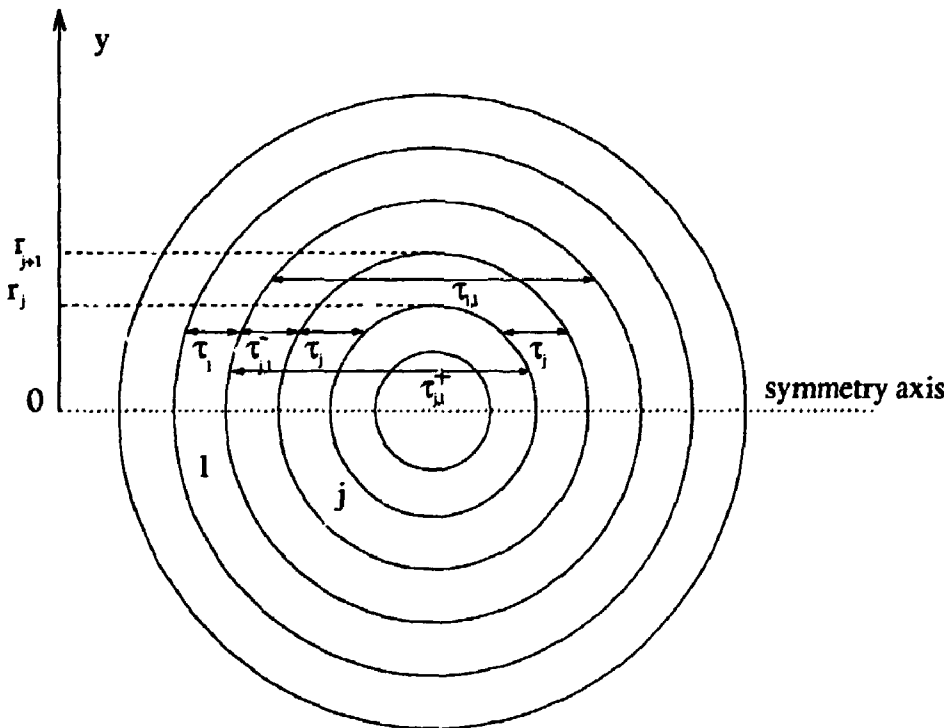


Figure 2.5 Calculation of collision probabilities in cylinder-geometry.

The total collision probability  $P_{j,i}$  is obtained by multiplying equation 19 by the differential area  $a \cdot dy'$  and the differential angle  $d\alpha$ , integrating over  $y'$  and  $\alpha$  and dividing the result by  $2 \cdot \pi \cdot V_i$ , where  $V_i$  is the cross sectional area of zone  $i$  ( $= \int a dy'$ ). In the case of reentrant bodies  $P_{j,i}(y')$  might consist of several contributions.

Finally, we consider the cylinder-symmetric case of figure 2.5. Because of rotational symmetry the integration over  $\alpha$  is not necessary and because of specular symmetry the integration over  $y$  is only necessary in the upper half of figure 2.5.

The reciprocity theorem is gratefully used for the calculation of the collision probabilities:

$$\Sigma_{t_l} \cdot V_l \cdot P_{j,l} = \Sigma_{t_j} \cdot V_j \cdot P_{l,j}. \quad (20)$$

This means that only collision probabilities with  $l \geq j$  have to be calculated by Carlvik's method. The probability  $P_{j,l}$  for a neutron from a spatially flat isotropic source in zone  $l$  to collide in zone  $j$  is given by:

$$\begin{aligned} 0.5 \cdot \Sigma_{t_l} \cdot V_l \cdot P_{j,l} = & \quad (21) \\ & \int_0^{r_j} [K i_3(\tau_{j,l}^-) - K i_3(\tau_{j,l}^- + \tau_1) - K i_3(\tau_{j,l}^- + \tau_j) + K i_3(\tau_{j,l}^- + \tau_1 + \tau_j)] dy + \\ & \int_0^{r_j} [K i_3(\tau_{j,l}^+) - K i_3(\tau_{j,l}^+ + \tau_1) - K i_3(\tau_{j,l}^+ + \tau_j) + K i_3(\tau_{j,l}^+ + \tau_1 + \tau_j)] dy + \\ & \int_{r_j}^{r_{j+1}} [K i_3(\tau_{j,l}^-) - K i_3(\tau_{j,l}^- + \tau_1) - K i_3(\tau_{j,l}^- + \tau_j) + K i_3(\tau_{j,l}^- + \tau_1 + \tau_j)] dy. \end{aligned}$$

The collision probability  $P_{j,j}$  takes a somewhat different form and is given by:

$$\begin{aligned} \Sigma_{t_j} \cdot V_j \cdot P_{j,j} = & \quad (22) \\ & \Sigma_{t_j} \cdot V_j - 4 \cdot \int_0^{r_j} [K i_3(0) - K i_3(\tau_j)] dy - \\ & 2 \cdot \int_{r_j}^{r_{j+1}} [K i_3(0) - K i_3(\tau_j)] dy + \\ & 2 \cdot \int_0^{r_j} [K i_3(\tau_{j,j}) - 2 \cdot K i_3(\tau_{j,j} + \tau_j) + K i_3(\tau_{j,j} + 2 \cdot \tau_j)] dy. \end{aligned}$$

The integral is split into intervals  $r_j < y < r_{j+1}$  and in every interval the Gaussian quadrature method is used. Consider the Gaussian quadrature formula:

$$\int_a^b f(y) dy = \frac{b-a}{2} \cdot \sum_{i=1}^n w_i \cdot f(x_i), \quad (23)$$

$$x_i = b - (b-a) \cdot \left(\frac{u_i}{2} + 0.5\right), \quad (24)$$

where  $u_i$  are the roots of the Legendre polynomial of the  $n^{\text{th}}$  degree and  $w_i$  are the weights as given by the Gaussian quadrature formula:

$$w_i = \frac{1}{P_n'(u_i)} \cdot \int_{-1}^{+1} \frac{P_n(u)}{u - u_i} \cdot du. \quad (25)$$

It is convenient to use  $u_i' = \frac{u_i}{2} + 0.5$  as Gauss-points and  $w_i' = \frac{w_i}{2}$  as Gauss-weights. These values are given in table 2.1 for quadratures with  $n$  ranging from 1 to 5.

$f(y)$  behaves as a regular function of  $\sqrt{b-y}$  in the neighbourhood of  $y \approx b$  which suggests to use the transformation  $u_i'' = u_i'^2$ . The integral is then given by:

$$\int_a^b f(y) dy = (b-a) \cdot \sum_{i=1}^n 2 \cdot u_i' \cdot w_i' \cdot f(x_i), \quad (26)$$

number of Gauss-points	Gauss-point $u'_i$	Gauss-weight $w'_i$
1	0.5	1.0
2	0.78867514	0.5
	0.21132486	0.5
3	0.5	0.44444444
	0.88729834	0.27777778
	0.11270166	0.27777778
4	0.33000948	0.32607258
	0.66999052	0.32607258
	0.93056816	0.17392743
	0.06943184	0.17392743
5	0.5	0.28444444
	0.76923466	0.23931434
	0.23076534	0.23931434
	0.95308993	0.11846345
	0.04691007	0.11846345

Table 2.1 Gauss-points and Gauss-weights.

where  $x_i = b - (b - a) \cdot (u'_i)^2$ . ROLAIDS-CPM has the option to choose the number of Gauss-points. The maximum number is 5.

So far, the collision probabilities are valid for a black boundary. However, a white boundary is used in cylinder-geometry.

The collision probability  $P_{j,l}^{\text{white}}$  is given by:

$$\begin{aligned}
 P_{j,l}^{\text{white}} &= P_{j,l}^{\text{black}} + P_{o,l} \times P_{j,o} + P_{o,l} \times P_{o,o} \times P_{j,o} + \\
 &\quad P_{o,l} \times (P_{o,o})^2 \times P_{j,o} + \dots \\
 &= P_{j,l}^{\text{black}} + \frac{P_{o,l} \times P_{j,o}}{(1 - P_{o,o})}, \quad (27)
 \end{aligned}$$

where the subscript o stands for the world outside the boundary of the cell.  $P_{o,l}$ ,  $P_{l,o}$ , and  $P_{o,o}$  are given by the conservation law and the reciprocity theorem as:

$$P_{o,l} = 1 - \sum_j P_{j,l}^{\text{black}}, \quad (28)$$

$$P_{j,o} = \frac{\sum_{t_j} \times V_j \times P_{o,j}}{\sum_{t_o} \times V_o}, \quad (29)$$

and

$$P_{o,o} = 1 - \sum_l P_{l,o}. \quad (30)$$

With the vector  $R_l$  defined as:

$$R_l = \sum_{t_l} \cdot V_l - \sum_j \sum_{t_j} \cdot V_j \cdot P_{j,l}^{\text{black}}, \quad (31)$$



it can easily be shown that:

$$\Sigma_{t_i} \cdot V_i \cdot P_{j,i}^{\text{white}} = \Sigma_{t_i} \cdot V_i \cdot P_{j,i}^{\text{black}} + R_i \cdot R_j \cdot \left( \sum_l R_l \right)^{-1}. \quad (32)$$

## 2.5 Calculation of effective cross sections

The flux at energy  $i$  in zone  $l$  is given by:

$$\phi_{i,l} = \frac{C_{i,l}}{\Sigma_{t_{i,l}} \cdot V_l}. \quad (33)$$

The group-averaged or effective cross sections follow from:

$$\sigma_{\text{eff}} = \frac{\int_E \int_V \sigma(E) \cdot \phi(E, r) dV dE}{\int_E \int_V \phi(E, r) dV dE}. \quad (34)$$

These cross sections are calculated for so-called "superzones" which are defined as contiguous zones with the same composition. ROLAIDS-CPM has the option to specify each zone as a superzone which means that zone-dependent group-averaged cross sections are calculated.

An extra option of ROLAIDS-CPM is the possibility to specify for which nuclides effective cross sections have to be calculated.

Not only does ROLAIDS produce "one-dimensional" effective cross sections, but also effective transfer matrix elements up to a given Legendre order are calculated. The group to group Legendre coefficients of the transfer matrix are defined as:

$$\sigma_l(g' \rightarrow g) \equiv \frac{\int_V \int_{E_g}^{E_{g-1}} \int_{E_{g'}}^{E_{g'-1}} \phi_l(E', r) \cdot \sigma_l(E' \rightarrow E) dE' dE dV}{\int_V \int_{E_{g'}}^{E_{g'-1}} \phi_l(E', r) dE' dV}, \quad (35)$$

where  $\phi_l(E, r)$  are the Legendre coefficients for the angular flux distribution. This  $\phi_l(E, r)$  is in ROLAIDS approximated by the scalar flux. The evaluation of equation 35 is done according to [12].

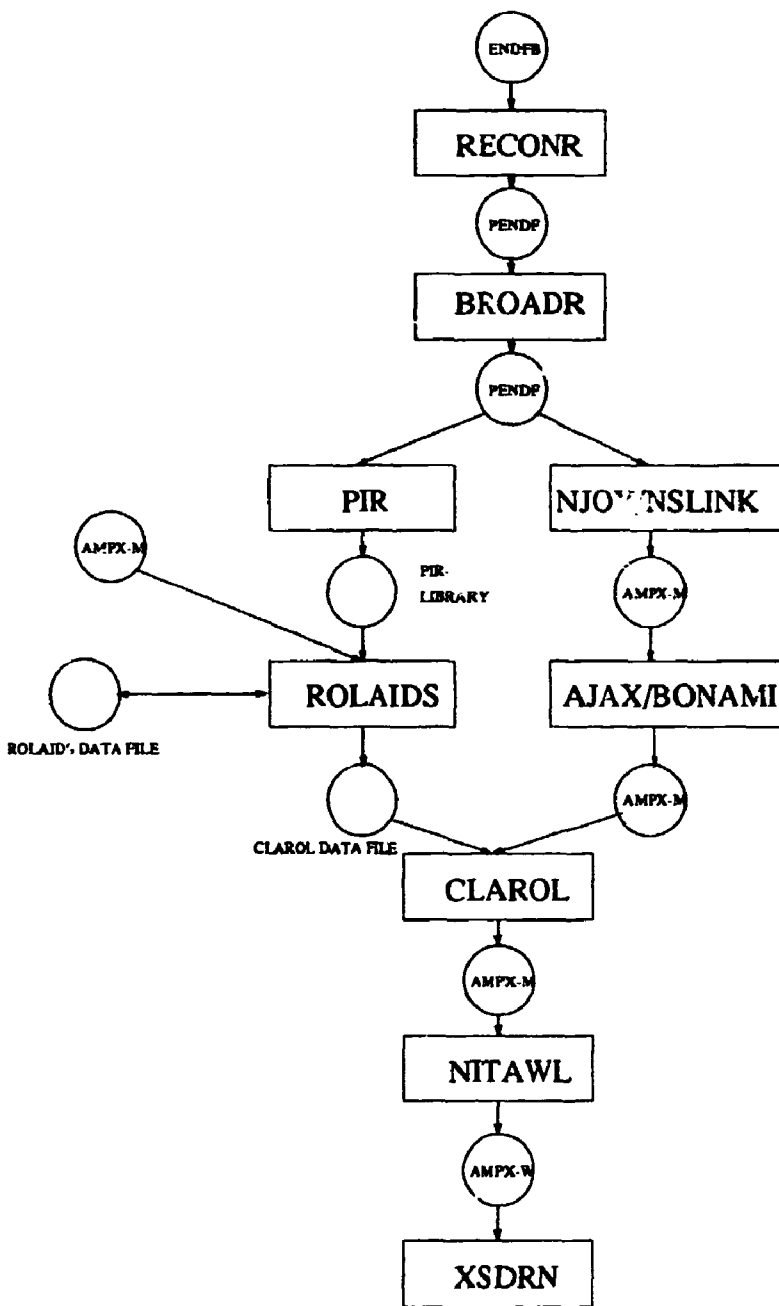


Figure 3.1 Position of ROLAIDS-CPM in the code system.

### 3. POSITION OF ROLAIDS-CPM IN CODE SYSTEM

ROLAIDS-CPM can be used in two different ways. First, it can be used to calculate the reaction rates in the resolved energy-range directly. Second, it can be used to calculate effective cross sections for a subsequent multigroup transport calculation. The usage of effective cross sections in the multigroup transport calculation creates the possibility to investigate the influence of higher order scattering terms which are neglected in ROLAIDS.

Figure 3.1 shows the position of ROLAIDS-CPM in the code system. The changes to the code system and a description how to use the code are given in this chapter.

Originally, ROLAIDS needs NPTXS [8] to generate the energy-pointwise cross

sections from the Evaluated Nuclear Data File (ENDF) [13]. An NPTXS library looks very much like the file 3 data in a PENDF file from NJOY [14]. PIR, which is an acronym for Produce Input library ROLAIDS-CPM, converts the PENDF file from the NJOY module BROADR to the required input library for ROLAIDS-CPM. PIR asks for the energy-range for which the PIR-library has to be made. This offers the opportunity to work with small libraries, while looking at specific energy-ranges. The PIR-library for ROLAIDS-CPM is described in table 3.1. It differs from the input library for the original ROLAIDS because the temperature of the nuclide is present in the first record. It has been interchanged with ZA.

Before performing the slowing down calculation ROLAIDS makes a data file which contains all the necessary information for a slowing down calculation with the selected nuclides.

ROLAIDS reads the energy group-structure for which the effective cross sections have to be calculated from an AMPX-M. The effective cross sections and the effective transfer matrix elements are written on a CLAROL data file which is a very long input file for CLAROL. CLAROL replaces the cross sections which are present on an AMPX-M for the specified nuclides by the effective cross sections which have been calculated by ROLAIDS. CLAROL extends the nuclide identification number MAT with the number of the superzone for which effective cross sections have been calculated.

NITAWL turns the AMPX-M into an AMPX-W. The cell-code XSDRN performs the cell calculation and produces cell weighted cross sections on an AMPX-W for further use by other codes [15].

The reaction rates in the different zones for the different energy groups can be extracted from the ROLAIDS output file by multiplying the effective cross sections by the group fluxes. They can also be extracted from the balance tables in the XSDRN output file. Note that the output and input files for the different modules are not given in figure 3.1.

Instead of writing effective cross sections to a CLAROL data file, ROLAIDS has the possibility to write the energy-pointwise flux distribution by zone to a data file. This possibility is also not shown in figure 3.1.

record	variable	description
1	MAT	identification number for nuclide
	MF	file number, always 3
	MT	reaction type 2 for elastic scattering 18 for fission 102 for radiative capture
	TEMP	temperature [K]
	AWR	atomic weight ratio
	IF	not used
	LFS	flag for broadened data
	IF	not used
	IF	not used
	2	MAT
MF		file number
MT		reaction type
ZA		100C · proton number Z + mass number A
Q		reaction Q-value (eV)
IF		not used
IF		not used
N1		number of interpolation types
N2		number of energy-points
NBT(1)		number of energy-points with interpolation type 1
JNT(1)		interpolation type 1
NBT(2)		number of energy-points with interpolation type 2 + NBT(1)
JNT(2)		interpolation type 2
....		....
NBT(N1)		N2
JNT(N1)		interpolation type N1 in our case with linearized PENDF files, N1=1,NBT(1)=N2,JNT(1)=2
E(1)		first energy point (eV)
$\sigma(1)$		first cross section value (b)
...		.....
E(i)		i <sup>th</sup> energy point (eV)
$\sigma(i)$	i <sup>th</sup> cross section value (b)	
...	.....	
E(N2)	last energy point (eV)	
$\sigma(N2)$	last cross section value (b)	
3	MAT	identification number for nuclide
	MF	file number
	0	7 times
RECORD 1-3 are repeated for IR reaction types		
IR*3+1	MAT	identification number for nuclide
	0	8 times end of data for this nuclide
IR*3+2	0	9 times

Table 3.1 Structure of the PIR-library for ROLAIDS-CPM.

# 4. INPUT DESCRIPTION

## 4.1 Introduction

This chapter gives the complete input prescription of the ROLAIDS-CPM program. The input parameters which are new or which have been changed compared to the original ROLAIDS program have been printed in a bold type style. The number of input parameters per array is given in square brackets.

## 4.2 Data Block 1

### 4.2.1 0\$\$ Array[10]

1..10 Logical number of devices N1 — N10

logical number	default value	purpose
N1	31	First PIR-library
N2	32	Second PIR-library
N3	16	Scratch device
N4	18 if IPRB $\geq$ 0 29 if IPRB < 0	Scratch device
N5	5	Card input device
N6	6	Printed output device
N7	29	ROLAIDS data file
N8	18	Scratch device
N9	9	Direct acces device
N10	26	if IPRB = 0: device for possible restart file if IPRB $\neq$ 0 and ICON $\neq$ 6: CLAROL data file if IPRB $\neq$ 0 and ICON = 6: Energy-pointwise flux distribution file

#### 4.2.2 I\$\$ Array[6]

1. **IGE** - problem geometry  
 0 - homogeneous  
 1 - slab  
 2 - cylinder  
 3 - sphere
2. **IZM** - number of zones for the integral transport calculation
3. **IM** - number of spatial intervals (may for convenience be chosen as the number of intervals in XSDRNPM)
4. **IBL** - the boundary condition at the left-hand boundary of the system  
 0 - vacuum (only IGE=1), interface-currents method  
 1 - interface-currents method  
   isotropic reflection (for IGE=1)  
   specular reflection (for IGE=2,3)  
 2 - periodic, interface-currents method (only IGE=1)  
 3 - periodic, collision probability method  
   (only IGE=1 and IBR=3)  
 4 - specular reflection, collision probability method  
   (only IGE=1,2 and IBR=4)
5. **IBR** - the boundary condition at the right-hand boundary of the system  
 0 - vacuum, interface-currents method  
 1 - isotropic reflection, interface-currents method  
 2 - periodic, interface-currents method (only IGE=1)  
 3 - periodic, collision probability method  
   (only IGE=1 and IBR=3)  
 4 - collision probability method (only IGE=1,2 and IBL=4)  
   specular reflection (for IGE=1)  
   isotropic reflection (for IGE=2)
6. **IPRB** - problem type  
 1 - create a ROLAIDS data file and perform a slowing down calculation  
 0 - create a ROLAIDS data file  
 -1 - mount a ROLAIDS data file and perform a slowing down calculation  
 -2 - mount a ROLAIDS data file and a problem restart file and complete a slowing down calculation

## 4.2.3 2\$\$ Array[8]

1. NDF1 - number of nuclides to be picked from PIR-library on N1
2. NDF2 - number of nuclides to be picked from PIR-library on N2
3. NMAST - not used
4. NFLAT - number of nonresonance nuclides treated with specified constant scattering cross section and a  $\frac{1}{v}$  absorption cross section
5. NSC - if NSC = 0 energy mesh based on maximum energy loss in a scattering collision with the heaviest nuclide is included ( $\alpha_{\max} \cdot E$ )  
- if NSC  $\neq$  0 energy mesh based on half of the above described energy loss is included (default=1)
6. ISR - if ISR = 0 a  $\frac{1}{E^{2.2}}$  flux above EHI is used as source  
- if ISR  $\neq$  0 a  $\frac{1}{E}$  source normalized to 1 is used in the zones with number  $\geq$  ISR (default=0) (only IBL  $\geq$  3)
7. MXX - number of compositions used in the problem mockup
8. MS - number of entries in the mixing table which specifies the makeup of the MXX compositions
9. ICON - print control for weighted one-dimensional cross sections  
7 - superzone weighted cross sections are printed  
6 - energy-pointwise fluxes by zone are put on N10  
5 - superzone, region, zone, cell  
4 - superzone, region, zone  
3 - superzone, region, cell  
2 - superzone, zone, cell  
1 - superzone, region  
0 - superzone, zone  
-1 - superzone, cell  
-7 - none
10. MASTU - Unit number of the AMPX-M input library (default = 28)
11. NSZ - if NSZ = 0 the superzones are a set of neighbouring zones with the same mixture number NMZ  
- if NSZ  $\neq$  0 every zone becomes a superzone which means that zone averaged cross sections are written on the CLAROL data file (default=0)
12. NGAU - the order of the Gauss quadrature to be used in the calculation of the collision probabilities in a cylinder-geometry (IGE=2,IBL=IBR=4) (default=5)

## 4.2.4 3\$\$ Array[2]

1. ISCT - the Legendre expansion order for the transfer matrix
2. MM - not used

#### 4.2.5 4\$\$ Array[6]

1. ELO - minimum problem energy (eV)  
When ELO is less than the energy below which thermal upscattering occurs on the AMPX-M, ELO becomes this last energy
2. EHI - maximum problem energy (eV)
3. EZP - if ISR = 0: magnitude of negative exponent of assumed flux above EHI (default=1.0)  
- if ISR  $\neq$  0: minimum energy of spatially flat  $\frac{1}{E}$  source
4. TK - temperature for thermal Maxwellian, used only if ICON=6 (default=0.0)
5. TE - time estimate, used to terminate slowing down calculation and generate a restart file, not used if TE=0.0 (default=0.0)
6. RQEPS - value used to set up energy mesh in the ROLAIDS data file, see equation 1 (default=1.0E-5)

T Terminate Data Block 1.

#### 4.3 Data Block 2

- 5\*\* RI(I=1,IM+1) - mesh boundaries from left to right (cm)
- 6\$\$ NZI(I=1,IM) - zone numbers by interval
- 7\$\$ NMZ(I=1,IZM) - mixture numbers by zone
- 9\*\* TN(I=1,NMT) - temperature of the nuclide  
(NMT=NDF1+NDF2+NFLAT)
- 10\$\$ ICH(I=1,NMT) - indicates if superzone weighted cross sections for this nuclide are put on the CLAROL data file (yes if ICH(I)  $\neq$  0, no if ICH(I)=0)
- 11\$\$ ID(I=1,NMT) - identification number of the nuclides in order of NDF1,NDF2,NFLAT
- 13\$\$ NM(I=1,MS) - mixture numbers of the nuclides in the mixing table
- 14\$\$ NID(I=1,MS) - nuclide identification number in the mixing table
- 15\*\* DNM(I=1,MS) - nuclide density in the mixing table
- 16\*\* TNN(I=1,MS) - nuclide temperature in the mixing table
- 17\*\* SSF(I=1,NFLAT) - constant scattering cross section for the NFLAT nuclides
- 18\*\* SCF(I=1,NFLAT) - thermal (0.025 eV) capture cross section for the NFLAT nuclides
- 19\*\* SFF(I=1,NFLAT) - thermal (0.025 eV) fission cross section for the NFLAT nuclides
- 20\*\* FA(I=1,NFLAT) - atomic weights for the NFLAT nuclides  
(used to be in 16\*\* array)

T Terminate Data Block 2



## 5. CONCLUSION

ROLAIDS performs an energy-pointwise slowing down integral transport calculation in one-dimensional geometry. It produces group-averaged cross sections. Because ROLAIDS assumes elastic scattering, the highest energy for which ROLAIDS can be used is limited by the onset of inelastic scattering. At low energies ROLAIDS is limited by thermal upscattering. It should also be noted that ROLAIDS assumes that radiative capture is the only important contribution to the disappearance of neutrons.

ROLAIDS uses the interface-currents method which assumes isotropic and spatially flat scattering sources in the different zones and cosine currents at the interfaces of the zones. The assumption of cosine currents at the interfaces of the boundaries is a serious physical limitation of the code. Therefore, the collision probability method has been implemented in ROLAIDS-CPM for the slab and cylinder-geometries. This method does not need any assumption about the currents at the interfaces of the zones. With the collision probability method accurate resonance absorption calculations are possible from the energy-pointwise cross sections.

The assumption of spatially flat scattering sources is not a physical limitation because more zones can be defined. The assumption of isotropic scattering sources is not expected to have much effect on resonance absorption calculations. The influence of this assumption for specific problems can be investigated with multigroup lattice codes.

Some useful options in ROLAIDS-CPM which are not present in ROLAIDS are described in this report. Up to now not much effort has been done to make the code user-friendly.

ROLAIDS-CPM will be placed at the disposal of the NEA data bank.

## References

- [1] N.M. Greene, "BONAMI-S: Resonance Self-Shielding by the Bondarenko Method," NUREG/CR-0200, Volume 2, Section F1, ORNL/NUREG/CSD-2/V2, 1981.
- [2] R.M. Westfall, I.M. Petrie, N.M. Greene & J.L. Lucius, "NITAWL-S: Scale System Module for Performing Resonance Shielding and Working Library Production," NUREG/CR-0200, Volume 2, Section F2, ORNL/NUREG/CSD-2/V2, 1981.
- [3] M.J. Roth, "The WIMS-E Modules W-PRES and W-RES," Atomic Energy Establishment, Winfrith, Dorset, AEEW - R 1707, 1983.
- [4] M.J. Roth, "Resonance Absorption in Complicated Geometries," Atomic Energy Establishment, Winfrith, Dorset, AEEW - R 921, 1974.
- [5] R. Sanchez, M. Coste, Z. Stankovski & C. van der Gucht, "Models for Multi-group Selfshielded Cross Sections Calculations in the Code APOLLO-II," *International Conference on the Physics of Reactors: Operation, Design and Computation 3* (1990), II-149 - II-163.
- [6] R.M. Westfall & M.A. Bjerke, "An Interface-Currents Integral Treatment for Treating Doubly Heterogeneous Multisystem Geometries," *Proceedings of the Topical Meeting on Computational Methods in Nuclear Engineering II* (1979), 7-71.
- [7] P.H. Kier & A.A. Robba, "RABBLE, A Program for Computation of Resonance Absorption in Multiregion Reactor Cells," Argonne National Laboratory, ANL-7326, 1967.
- [8] N.M. Greene, J.L. Lucius, L.M. Petrie, W.E. Ford, J.E. White & R.Q. Wright, "AMPX: A Modular Code System for Generating Coupled Multigroup Neutron Gamma Libraries from ENDF/B," ORNL/TM-3706, 1976.
- [9] H. Tellier, M. Coste, C. Raepsaet & C. Van der Gucht, "Heavy Nucleus Resonant Absorption Calculation Benchmarks," *Nuclear Science and Engineering* 113 (1993), 20-30.
- [10] I. Carlvik, "A method for Calculating Collision Probabilities in General Cylindrical Geometry and Applications to Flux Distributions and Dancoff Factors," *International Conference on the Peaceful Use of Atomic Energy 3* (1964), P/681.
- [11] W.G. Bickley & J. Nayler, "A Short Table of the Functions  $K_i(x)$ , from  $n=1$  to  $n=16$ ," *Phil. Mag.* 20 (1935), 343-347.
- [12] J.A. Bucholz, "An Analytical Angular Integration Technique for Generating Multigroup Transfer Matrices," *Nucl. Sc. And Eng.* 74 (1980), 163-167.

- 
- [13] R. Labauve, C. Lubitz, R. Macfarlane, S. Pearlstein, R. Peelle, R. Roussin & L. Stewart, "ENDF-102 Data Formats and Procedures for the Evaluated Nuclear Data File ENDF-6," BNL-NCS 44945, 1990 (Revised 10/91).
- [14] R.E. MacFarlane, D.W. Muir & R.M. Boicourt, "The NJOY Nuclear Data Processing System," Los Alamos National Laboratory, LA-9303-M (ENDF 324), 1982.
- [15] L.M. Petrie & N.M. Greene, "XSDRNPM: AMPX module with one dimensional  $S_n$  capability for spatial weighting.," ORNL/RSIC-PSR-63, 1978.